Accelerated Aiming Strategy in Central Receiver Systems Using Integer Linear Programming

Pascal Richter[1, a)], Nils Speetzen[1]

[1]RWTH Aachen University, Department of Computer Science, Ahornstr. 55, 52074 Aachen, Germany.

[a)]Corresponding author: pascal.richter@rwth-aachen.de

Abstract. Aiming strategies are used to distribute the heat flux on the receiver surface with the aim to maximize the mass flow of the heat transfer fluid in the receiver tubes while avoiding thermal overloading. The optimization problem is modeled as an integer program (IP) to provide deterministic solutions. To improve the runtime, several accelerations are investigated as the grouping of heliostats to reduce the size of the optimization problem. In a case study we show that an optimal solution can be found within seconds while maintaining high accuracy.

INTRODUCTION

In central receiver systems aiming strategies are used to align the heliostats to reach a desired flux distribution on the surface of the receiver. There already exist different approaches to find an optimal aiming strategy: [1] proposes a solution based on the ant colony optimization metaheuristic, [2] assumes that all heliostats aim at the center of the receiver to optimize a central receiver system as a whole, while [3] offers fixed approaches for aiming strategies. [4] uses a genetic algorithm and [5] uses linear programming to determine an optimal solution, which was in [6] extended to a robust approach. [1], [2] and [3] do not necessarily find an optimal aiming strategy due to their heuristic nature or the usage of a fixed strategy. [4], [5], and [6] need a large run-time such that they cannot be used for real-time application.

This work aims to achieve close to optimal results in real time, which means less than 10 seconds in dynamical situations of passing clouds. Therefore, the problem is formulated as linear problem (LP) while its size is reduced using moderate additional heuristic constraints to accelerate the search in the search tree.

FLUX DISTRIBUTION

The heliostat aiming strategy is represented by virtual aim points at the receiver surface, at which the heliostats can aim. For each heliostat and each reachable aim point the flux distribution on the receiver surface can be pre-computed. We use an extended version of the HFLCAL method from [6], which takes perspective stretching into account.

Each receiver has an upper limit for the heat flux hitting it, because its surface can only withstand a certain maximum temperature. Additionally, it might be desirable that a specific heat flux distribution is created at the receiver surface, which can depend on the layout of the tubes containing the heat carrying medium behind the receiver surface. Thus, for a $\mathrm{n}^{\mathrm{horiz}} \times \mathrm{n}^{\mathrm{vert}}$ array of receiver cells m we define the allowed flux distribution (AFD) with an allowed heat flux value $\mathrm{q}^{\mathrm{m,AFD}}$. A heliostat flux deviation above the AFD in any cell m could lead to damage the receiver, which needs to be prohibited.

The AFD values $\mathrm{q}^{\mathrm{m,AFD}}$ are given by the operator of the central receiver system, which mainly relies on an entirely different optimization problem: Since the AFD depends strongly on the current mass flow settings for the heat carrying medium, the operator has to find a balance between a high mass flow and a high temperature.

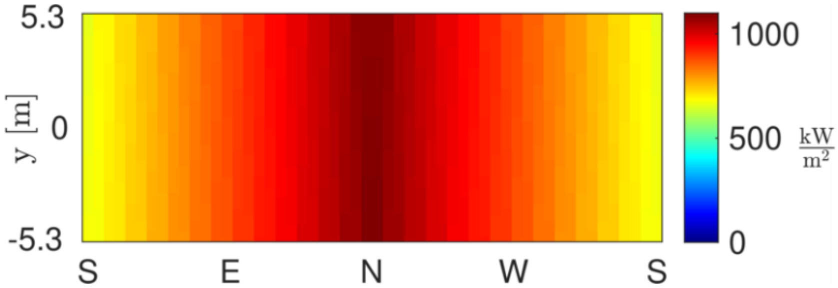

FIGURE 1. Example for an Allowed Flux Distribution (AFD) on the surface of a receiver with n^{horiz}=54 and n^{vert}=42 cells. The x-axis shows the cardinal direction (N=North, E=East, S=South and W=West).

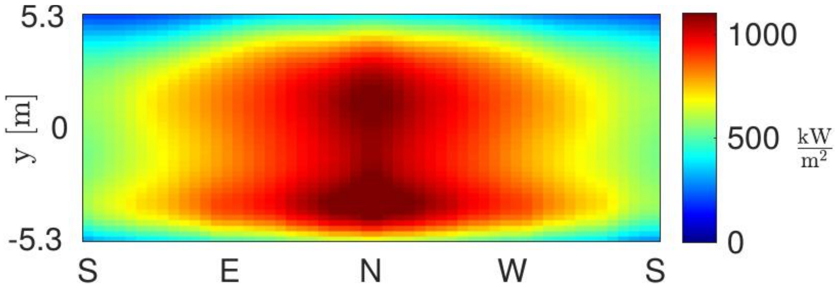

FIGURE 2. Example for a reached heat flux distribution on the surface of a receiver with n^{horiz}=54 and n^{vert}=42 cells. The x-axis shows the cardinal direction (N=North, E=East, S=South and W=West).

AIMING STRATEGY AS INTEGER LINEAR PROGRAM

The objective of the aiming strategy is to maximize the received flux on the receiver, while considering that in all receiver cells the received flux never exceeds the desired flux of the given AFD. The underlying optimization problem is formulated as a LP, where the binary decision parameters decide if a heliostat aims on an aim point or not. Beside the desired heat flux as an upper bound for the received heat flux, we also consider safety constraints for the heat shield around the receiver.

The objective of the optimization problem is to maximize the concentrated heat flux on the receiver surface,

$$\text{maximize} \sum_{m \in M^{\text{rec}}} (q^m \cdot A^m) . \tag{1}$$

For each receiver cell m with its area A^m the received flux is given by

$$q^m = \sum_{h \in H} \sum_{a \in A} q^m_{h,a} \cdot x_{h,a} \quad \forall m \in M \tag{2}$$

The notation $q^m_{h,a}$ describes the heat flux in receiver cell m from heliostat h aiming on point a. The heliostats H are allowed to aim at specific points at the receiver surface, called aim points from the set A. There exists one binary decision variable $x_{h,a}$ for each pair $(h, a), h \in H, a \in A$, which determines if the heliostat $h \in H$ targets the aim point $a \in A$, i.e.

$$x_{h,a} \in \{0,1\} \quad \forall h \in H \quad \forall a \in A \tag{3}$$

If heliostat h targets aim point a then $x_{h,a} = 1$, otherwise it is 0. A heliostat can aim at most on one aim point,

$$\sum_{a \in A} x_{h,a} \leq 1 \quad \forall h \in H \tag{4}$$

This enables the computation of solutions where some heliostats have to stay unused due to safety constraints.

A heliostat should only aim at aim points which can be reached, which is not always the case for cavity and external receivers. For a heliostat, we call the blocked aim points A_h^{blocked} and forbid the use of these points as a target. Thus, we set the decision parameters to these aim points to zero,

$$x_{h,a} \equiv 0 \quad \forall a \in A_h^{\text{blocked}} \tag{5}$$

The allowed flux distribution (AFD) $q^{m,\text{AFD}}$ in kW/m^2 serves as an upper limit for the total heat flux density at the measurement points. Its constraint is formulated as

$$\sum_{h \in H} \sum_{a \in A} q_{h,a}^{m} \cdot x_{h,a} \leq q^{m,\text{AFD}} \quad \forall m \in M^{\text{rec}} \tag{6}$$

A heat shield is installed at the edges of the receiver, to prevent damage to the solar tower from heat flux missing the receiver. This heat shield usually has a lower allowed heat flux than the receiver surface, therefore the heat flux at the edges of the receiver is constraint to q^{shield} in kW/m^2.

$$\sum_{h \in H} \sum_{a \in A} q_{h,a}^{m} \cdot x_{h,a} \leq q^{\text{shield}} \quad \forall m \in M^{\text{shield}} \tag{7}$$

To solve the integer linear program, we use Gurobi [7], a commercial optimizer solver software.

ACCELERATION USING HELIOSTAT GROUPING

To reduce the size of the optimization problem, the heliostats are organized into groups which target onto the same aim point. Thus, if we use groups with about c heliostats, then the number of decision parameters is reduced by factor c. Therefore, we call this parameter the compression factor c. The groups are composed in such a way that at most all of its heliostats can reach the same set of aim points (e.g. if we regard an external receiver the heliostats are all from a similar angular range). This is achieved using complete linkage agglomerative clustering with the angular difference of the heliostats from the receiver as the dissimilarity function, which results in groups of even sizes, where all heliostats can see almost exactly the same aim points, as long as c is not extraordinarily large.

It is clear that due to the grouping the quality of the solution decreases. In Fig. 3 it can be seen that the received flux for a compression factor of $c = 4$ reduces to about 98.99 %, in comparison to the optimal solution with $c = 1$. But at the same time the computational time is reduced by a factor of 4.2 on a standard PC, see Fig. 4. Using $c = 8$ we get an accuracy of 98.2 % and a speedup of 7.8.

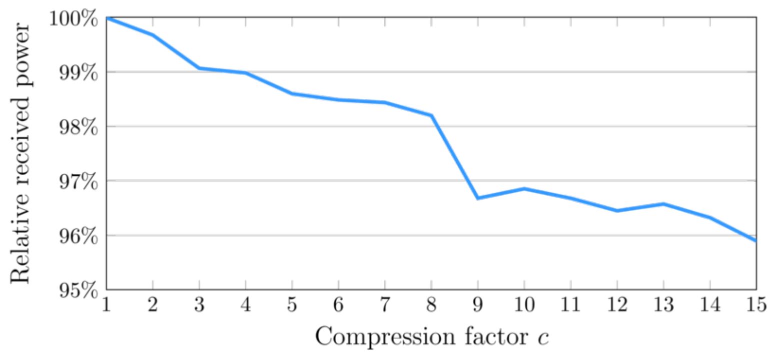

FIGURE 3. Quality of the solution in dependency of the grouping size, using the Gemasolar test case with 2650 heliostats and 135 aim points on the external receiver surface.

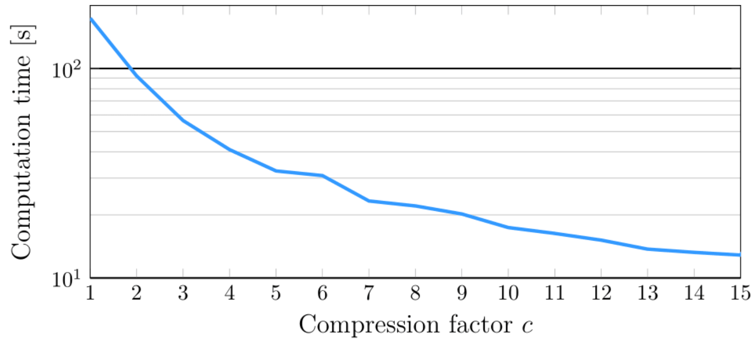

FIGURE 4. Runtime of the solution in dependency of the grouping size, using the Gemasolar test case with 2650 heliostats and 135 aim points on the external receiver surface.

The resulting heat flux distributions on the receiver surface using a compression factor of $c = 1$ and $c = 4$ are drawn in Fig. 5 and Fig. 6. As just minor differences can be seen, a comparison between both images is shown in Fig. 7.

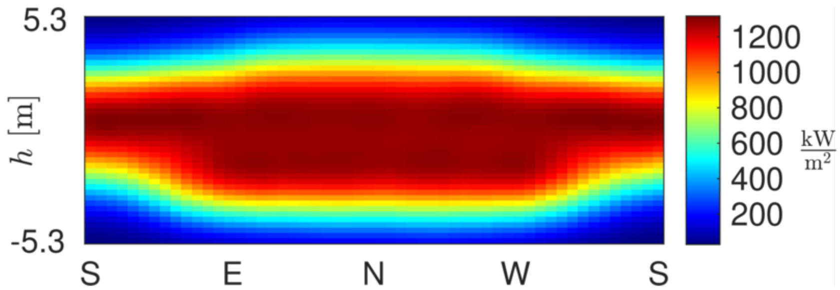

FIGURE 5. Heat flux distribution on the receiver surface of the solution with $c = 1$ in dependency of the grouping size, using the Gemasolar test case with 2650 heliostats and 135 aim points on the external receiver surface.

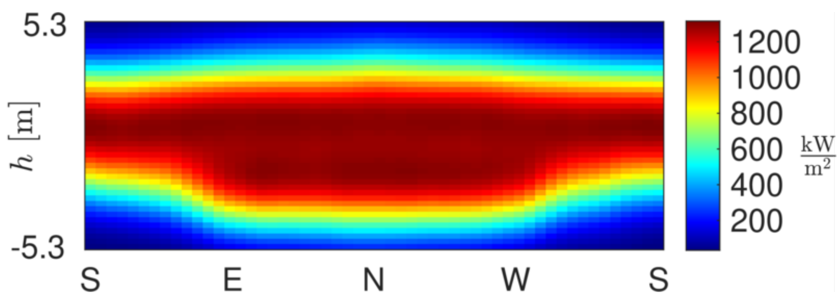

FIGURE 6. Heat flux distribution on the receiver surface of the solution with $c = 4$ in dependency of the grouping size, using the Gemasolar test case with 2650 heliostats and 135 aim points on the external receiver surface.

The resulting aim point assignment can be seen in Fig. 8 for a compression factor $c = 1$ and in Fig. 9 for $c = 4$. It can be seen that the outer heliostats tend to aim towards the center of the receiver in the default solution, while inner heliostats aim at different aim points closer to the border of the receiver. Applying the grouping forces some of the outer heliostats to aim at outer receiver points and inner heliostats at central points, as the grouping is done radially without consideration for the distances from the receiver. Even though, the changes in the resulting heat flux image are little.

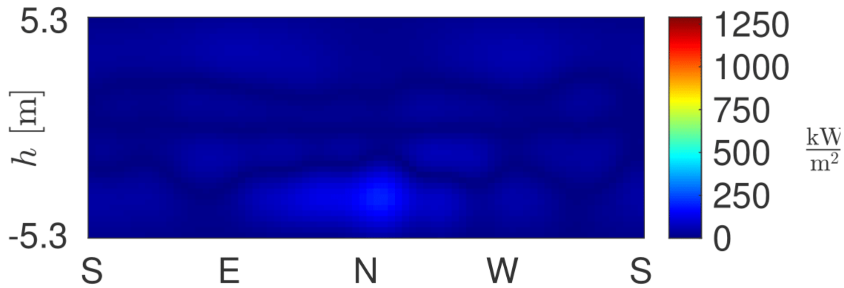

FIGURE 7. Absolute difference in heat flux distribution on the receiver surface between the solutions with $c = 1$ and $c = 4$ in dependency of the grouping size, using the Gemasolar test case with 2650 heliostats and 135 aim points on the external receiver surface.

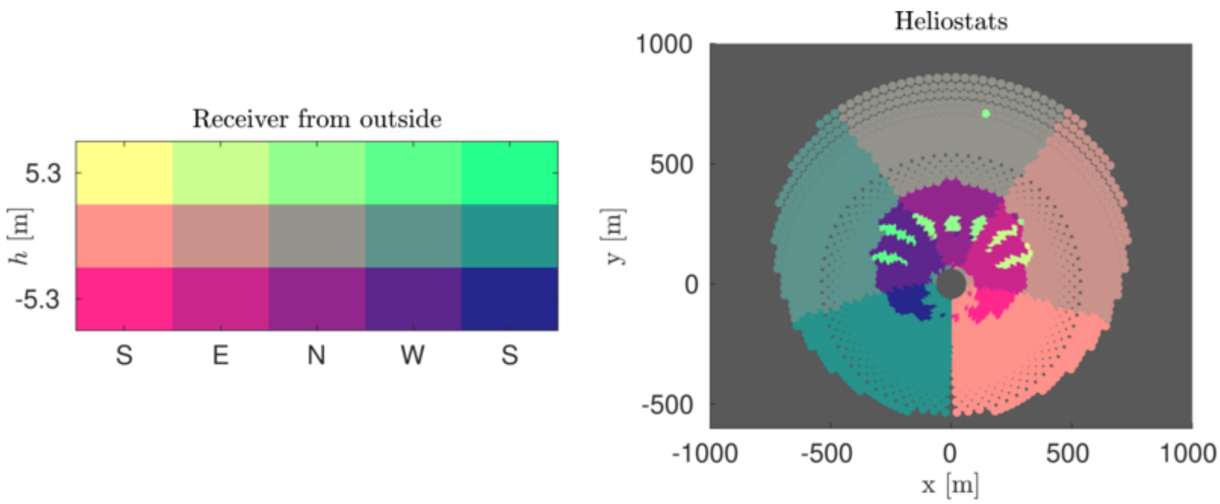

FIGURE 8. Aim point assignment with a compression factor $c = 1$, using the Gemasolar test case with 2650 heliostats and 135 aim points on the external receiver surface.

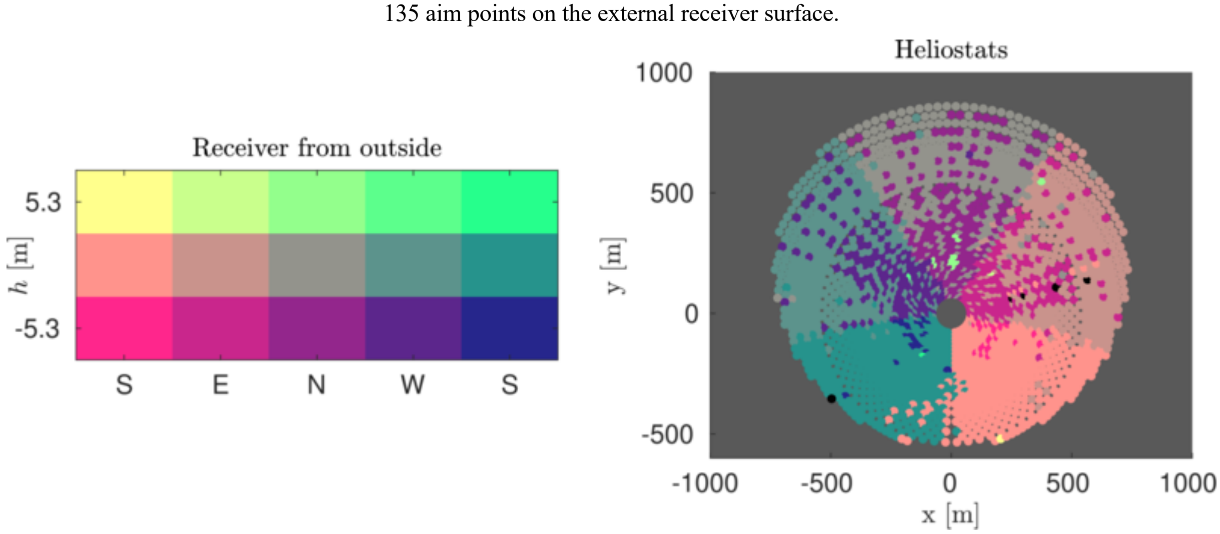

FIGURE 9. Aim point assignment with a compression factor $c = 4$, using the Gemasolar test case with 2650 heliostats and 135 aim points on the external receiver surface.

Altogether, the results of the LP with a compression factor of $c = 4$ give comparable results, while accelerating the runtime by a factor of 4.2.

CONCLUSION

For real-world applications, a low run-time of the heliostat aiming strategy optimization is essential. The presented method can reduce the runtime of the exact solution process significantly while staying very close to the global optimum for standard power plants. The method can be extended to arbitrary receiver and heliostat types as well as arbitrary heliostat field layouts. The next steps are further reductions of the computational time when using initial solutions. This is the case when dynamic test cases with cloud movements are regarded.

REFERENCES

1. Belhomme, B., Pitz-Paal, R., & Schwarzbözl, P. (2014). Optimization of heliostat aim point selection for central receiver systems based on the ant colony optimization metaheuristic. *Journal of solar energy engineering*, *136*(1), 011005.
2. Carrizosa, E., Domínguez-Bravo, C., Fernández-Cara, E., & Quero, M. (2015). A heuristic method for simultaneous tower and pattern-free field optimization on solar power systems. *Computers & Operations Research*, *57*, 109-122.
3. Astolfi, M., Binotti, M., Mazzola, S., Zanellato, L., & Manzolini, G. (2017). Heliostat aiming point optimization for external tower receiver. *Solar Energy*, *157*, 1114-1129.
4. Besarati, S. M., Goswami, D. Y., & Stefanakos, E. K. (2014). Optimal heliostat aiming strategy for uniform distribution of heat flux on the receiver of a solar power tower plant. *Energy Conversion and Management*, *84*, 234-243.
5. Ashley, T., Carrizosa, E., & Fernández-Cara, E. (2017). Optimisation of aiming strategies in Solar Power Tower plants. *Energy*, *137*, 285-291.
6. Kuhnke, S., Richter, P., Kepp, F., Cumpston, J., Koster, A. M., & Büsing, C. (2020). Robust optimal aiming strategies in central receiver systems. *Renewable Energy*, 152, 198-207.
7. LLC Gurobi Optimization. Gurobi optimizer reference manual, 2020. URL http://www.gurobi.com. last visited on 08.09.2020